

Article

Co-Gasification of Pistachio Shells with Wood Pellets in a Semi-Industrial Hybrid Cross/Updraft Reactor for Producer Gas and Biochar Production

Jiří Ryšavý ^{1,*} , Jakub Čespiva ¹ , Lenka Kuboňová ¹, Milan Dej ¹ , Katarzyna Szramowiat-Sala ² , Oleksandr Molchanov ¹, Lukasz Niedzwiecki ^{3,*} , Wei-Mon Yan ^{4,5} and Sangeetha Thangavel ^{4,5} 

- ¹ Energy Research Centre, Centre for Energy and Environmental Technologies, VSB—Technical University of Ostrava, 708 00 Ostrava, Czech Republic; jakub.cespiva@vsb.cz (J.Č.); lenka.kubonova@vsb.cz (L.K.); milan.dej@vsb.cz (M.D.); oleksandr.molchanov@vsb.cz (O.M.)
- ² Department of Coal Chemistry and Environmental Sciences, Faculty of Energy and Fuels, AGH University of Krakow, 30-059 Kraków, Poland; katarzyna.szramowiat@agh.edu.pl
- ³ Department of Energy Conversion Engineering, Wrocław University of Science and Technology, 50-370 Wrocław, Poland
- ⁴ Department of Energy and Refrigerating Air-Conditioning Engineering, National Taipei University of Technology, Taipei 10608, Taiwan; wmyan@ntut.edu.tw (W.-M.Y.); sangeetha@mail.ntut.edu.tw (S.T.)
- ⁵ Research Center of Energy Conservation for New Generation of Residential, Commercial and Industrial Sectors, National Taipei University of Technology, Taipei 10608, Taiwan
- * Correspondence: jiri.rysavý@vsb.cz (J.R.); lukasz.niedzwiecki@pwr.edu.pl (L.N.)

Abstract: The possibilities of pistachio shell biochar production on laboratory-scale gasification and pyrolysis devices have been described by several previous studies. Nevertheless, the broader results of the pistachio shell co-gasification process on pilot-scale units have not yet been properly investigated or reported, especially regarding the detailed description of the biochar acquired during the routine operation. The biochar was analysed using several analytical techniques, such as ultimate and proximate analysis (62%wt of C), acid–base properties analysis (pH 9.52), Fourier-transform infrared spectroscopy (the presence of –OH bonds and identification of cellulose, hemicellulose and lignin), Raman spectroscopy (no determination of Id/Ig ratio due to high fluorescence), and nitrogen physisorption (specific surface 50.895 m²·g^{−1}). X-ray fluorescence analysis exhibited the composition of the main compounds in the biochar ash (32.5%wt of Cl and 40.02%wt of Na₂O). From the energy generation point of view, the lower heating value of the producer gas achieved 6.53 MJ·m^{−3} during the co-gasification. The relatively high lower heating value of the producer gas was mainly due to the significant volume fractions of CO (6.5%_{vol.}), CH₄ (14.2%_{vol.}), and H₂ (4.8 %_{vol.}), while hot gas efficiency accomplished 89.6%.

Keywords: gasification; novel reactor; pistachio shell; biochar; waste management; sustainability



Citation: Ryšavý, J.; Čespiva, J.; Kuboňová, L.; Dej, M.; Szramowiat-Sala, K.; Molchanov, O.; Niedzwiecki, L.; Yan, W.-M.; Thangavel, S. Co-Gasification of Pistachio Shells with Wood Pellets in a Semi-Industrial Hybrid Cross/Updraft Reactor for Producer Gas and Biochar Production. *Fire* **2024**, *7*, 87. <https://doi.org/10.3390/fire7030087>

Academic Editor: Ali Cemal Benim

Received: 26 January 2024

Revised: 4 March 2024

Accepted: 7 March 2024

Published: 14 March 2024



Copyright: © 2024 by the authors. Licensee MDPI, Basel, Switzerland. This article is an open access article distributed under the terms and conditions of the Creative Commons Attribution (CC BY) license (<https://creativecommons.org/licenses/by/4.0/>).

1. Introduction

Gasification is one of the most feasible thermochemical processes, besides pyrolysis and torrefaction, for producing high-quality, sustainable, multi-purpose materials that can widely replace fossil fuel-based materials in many applications [1–3]. The equivalence ratio (ER) usually ranges from 0.1 to 0.5, while process temperatures are held between 650 and 1200 °C [4,5] depending on the gasification principle (fixed bed [6], fluidised bed [7], or entrained flow [8]). The gasification media includes air, steam, CO₂, or their mixtures [9–12]. The gasification process results in two major products: combustible gas (known as producer gas) and char (in case of biomass gasification biochar). Producer gas can be used as a fuel, e.g., in an Otto engine with consequent heat end power generation [13]. A more advanced method of producer gas application for production of added-value goods is its upgrading to syngas, along with subsequent application in chemical synthesis processes, especially in

the Fischer–Tropsch process for the production of liquid hydrocarbons [14]. However, an appropriate composition rate of H_2/CO must comply sufficiently, which is quite difficult without additional H_2 supply [15]. The resulting hydrocarbon chains may consequently be utilised as carbon-neutral fuel (in the case of biomass usage as the input feedstock to the gasification process), or can be employed as CCU/CCS medium [16]. Moreover, recent research studies proposed BECCS technologies with integrated gasification [17]. Hydrogen-rich gas is also attractive currently due to policies aiming to promote hydrogen use [18–20].

Biochar could be implemented in circular economy systems in many different techniques [21]. The most straightforward use involves the agricultural application of this nutrition-rich substance to the soil as a soil amendment procedure [22]. Other applications include mercury capture from flue gas [23], air purification [24], drinking or wastewater treatment [25], adsorption chiller filling [26], and capture of radioactive substances [27].

The *Pistacia vera* is a small tree which produces pistachio nuts. Global pistachio production has been on an upward trend for more than a decade, with 1.3 million tonnes of pistachios produced in 2021, according to the latest verified data [28]. The largest producers are Iran, the USA, Turkey, and China. In terms of weight, the shell weighs about 35–45 %wt of the whole nut, so 455–585 thousand tonnes of pistachio shells are produced annually. The pistachio nuts are usually sold in a shell directly to the final customers or for further processing by the companies (production of ice cream, flour, or flavourings).

The granulometry of the pistachio shells after the standard shelling process is very homogenous, and it could be mixed and directly used in appliances designed for pellets, as shown by Ryšavý et al. [29], which is important due to the energy required for the densification of biomass [30–32]. In the study of Hu et al. [33], pistachio shells were gasified under specific laboratory conditions, while the KOH-activated char was described in detail and tested for its capacitive performance in aqueous electrolytes in electric double-layer capacitors. The experimental results of Lua and Yang [34] showed that it is feasible to prepare activated carbons with a high specific surface (BET) area ($896 \text{ m}^2 \cdot \text{g}^{-1}$) and micropore volume ($0.237 \text{ cm}^3 \cdot \text{g}^{-1}$) from pistachio shells by means of vacuum pyrolysis and CO_2 activation. The impacts of pH, adsorbent dosage, and temperature on Acid Violet 17 dye removal was studied by Vijayalakshmi et al. [35] while using chemically prepared adsorbents from a pistachio nut shell. The effects of different parameters on pistachio shell char were investigated during pyrolysis (at temperature 400–700 °C) and consequent activation (at temperature 800–950 °C) from the specific surface areas point of view in the study of Faramazi et al. [36].

The majority of previous studies aimed at the thermal treatment of pistachio shells have used laboratory or small/bench-scale units, indicating the great potential of pistachio shells as input feedstock and the resulting biochar as a widely usable material. Most of the previously published research articles describing the quality of the solid residue after its thermal processing were mainly focused on the optimisation of the process to achieve the highest possible parameters in terms of downstream application without evaluating the energy parameters of the process. The potential of co-gasification of the pistachio shell on a semi-industrial scale with a cross/updraft gasification reactor has not been evaluated yet as far as the research knowledge of the authors is concerned. Having a comprehensive understanding of both the energy parameters of the process, as well as the detailed characterisation of the solid by-product, is necessary for the assessment of its suitability for various applications (use of the biochar as a soil amendment or as feedstock for subsequent activation). The novelty of the study presented herein lies in its pioneering exploration of pistachio shell co-gasification on a semi-industrial unit, the detailed characterization of producer gas and resulting biochar, and its potential applications within the context of the circular economy.

2. Materials and Methods

2.1. Feedstock

Pistachio shells were obtained from the supplier of Californian Pistachios with cores included (verified quality for consumption by a human). After the separation of the cores from the shells, they were stored in the laboratory for several months before the experiments, allowing the moisture content to reach equilibrium with ambient air in the building. For the gasification test, a mixture of pistachio shells with certified wood pellets of EN plus A1 quality was used in a weight ratio of 15/85 (pistachio shells/wood pellets).

2.2. Gasification—Pilot-Scale Rig and Gas Analysis

The technology utilised for the purpose of this research was based on a semi-industrial scale sliding bed gasification reactor equipped with a circular grate. The reactor scheme is presented in Figure 1. The fuel and oxidising media flows defined this reactor as a hybrid cross/updraft with a tangential oxidising media inlet. The reactor worked in an autothermal regime, which required no additional energy input from an external source. A more detailed description of the performance of this technology on wood biomass was included in the study of Čespiva et al. [37], on torrefied biomass in the study of Čespiva et al. [38], and on solid recovered fuel in another work of Čespiva et al. [39].

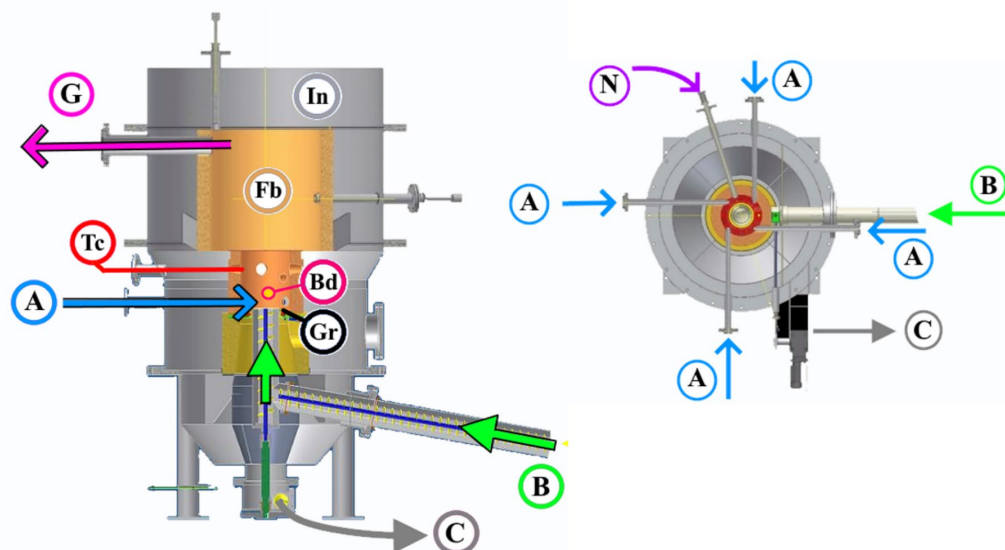


Figure 1. Cross/updraft gasification reactor with a sliding bed over circular grate [37]. Gr—circular grate; B—fuel input; Fb—freeboard; A—oxidising media input; G—producer gas output; C—residual char output; Bd—sliding bed; N—star-up flame pipe; Tc—thermocouple.

The experimental gasification process was held under a low load regime, with ER reaching only 0.205 (stoichiometric air need was 5.55 kg per kilogram of fuel), using air as the oxidising medium, while the fuel flow was equal to $7.2 \text{ kg}\cdot\text{h}^{-1}$. The gasification temperature was maintained between 625.4 and 704.7 °C during the entire duration of the experimental measurement, with an average value equal to 649.7 °C. The relative pressure within the reactor was -0.1 kPa . The producer gas composition, as well as its LHV, were determined by the Gas 3000p (Pollutek Gas Analysis, Belgium) gas analyser with NDIR, TCD, and ECD sensors for CO, H₂, CO₂, CH₄, C_nH_m, and O₂ detection. All measured values were determined for a dry gas, which passed through a series of 6 impinger bottles immersed in an ice bath before going through the analyser, allowing for the condensation of tars and moisture present in the gas.

Efficiency determination is a tool for the direct comparison of gasification processes regardless of reactor design type, fuel characteristics, and operating conditions. The hot gas efficiency (HGE) value presents the efficiency of converting the input chemical energy from

feedstock material to the energy of the producer gas, including its sensible heat, while the cold gas efficiency (CGE) does not include this value. These efficiencies were determined according to the following Equations (1) and (2) [40–42]:

$$\eta_{hg} = \frac{\dot{m}_g \times c_p \times \Delta T + \dot{m}_g \times LHV_g}{\dot{m}_f \times LHV_f} \quad (1)$$

$$\eta_{cg} = \frac{\dot{m}_g \times LHV_g}{\dot{m}_f \times LHV_f} \quad (2)$$

LHV_f—lower heating value of the feedstock [J·kg⁻¹];

LHV_g—lower heating value of the producer gas [J·kg⁻¹];

ΔT—temperature diff. between ambient temperature (293.15 K) and the actual temperature of the producer gas, measure at the outlet of the gasifier [K];

c_p—specific heat capacity at a constant pressure of the gas [J·(kg·K)⁻¹];

\dot{m}_f —mass flow rate of the feedstock [kg·h⁻¹];

\dot{m}_g —mass flow rate of the gas [kg·h⁻¹].

The mass flow of the feedstock was determined via calibration of the feeding auger for different rotations per minute (RPM), which could be set by the control system of the gasification installation. During the calibration, the auger was unplugged from the gasifier and fed the material to an empty container for 30 min. The mass of the container was checked before and after the feeding period, and the mass flow rate of the feedstock was subsequently calculated. The producer gas flow rate was measured using a measuring orifice. Pressure on both sides of the orifice was measured using Siemens Sitrans P pressure sensors with a 7MF4433 pressure transformer (Siemens AG Bereich Automatisierungs und Antriebstechnik Geschäftsgebiet Process Instrumentation, D-76181 Karlsruhe, Germany). The volumetric flow rate of the producer gas was recalculated to the mass flow rate based on the measured composition of the gas and the densities of each of the measured compounds. The air flow rate was measured using a Testo 6444 flow meter, operating according to the thermal (calorimetric) measuring principle and using a glass-coated ceramic sensor, with the response time lower than 0.1 s.

2.3. Analytical Methods for the Analysis of Feedstock and Obtained Biochars

The solid residue was collected from a drop zone below the reactor, subsequently separated (gasified pistachio shells, gasified wood pellets), and analysed. The contents of C, H, N, and S were determined using CHN628 and CHNS628 (both Leco, St. Joseph, MI, USA). The amount of O was calculated following the EN 16993 standard. The content of W was determined as a gravimetric difference in the VF110 electric furnace (Mettler, Germany) (ISO 181234-2). The ash content was determined in the LEO 5/11 furnace (LAC, Zidlochovice, Czech Republic) (ISO 18122). The lower heating value (LHV) was calculated according to the Equation (1) [43], using the HHV value obtained with the calorimeter AC600 (LECO, USA).

$$LHV = HHV - (k \times 8.94 \times \omega_H + 0.8 \times (\omega_N + \omega_O) + k_1 \times w) \quad (3)$$

k: heat of vaporization considering the volumetric work done by the water formed from the hydrogen during combustion at 25 °C, 2.37 MJ·kg⁻¹;

*k*₁: specific heat of water evaporation at constant pressure at 25 °C, 2.44 MJ·kg⁻¹;

ω_H : mass fraction of hydrogen in the fuel, [kg·kg⁻¹];

ω_N : mass fraction of the nitrogen in the fuel, [kg·kg⁻¹];

ω_O : mass fraction of the oxygen in the fuel, [kg·kg⁻¹];

ω_w : mass fraction of the water in the fuel, [kg·kg⁻¹].

The pH value was determined following the ISO 10523:2008 standard by using a pH meter, CyberScan pH 110 (EUTECH INSTRUMENTS, Singapore), with a detection range

from -2.00 to 16.00 pH. The material was dissolved in deionised water for 24 h prior to the measurement.

The ash from pistachio shell biochar was prepared by ashing the biochar at 550 °C for 4 h in an oven under an oxidation atmosphere for the purpose of XRF spectrometry analysis on a Xepos (SPECTRO, Kleve, Germany) device. Nicolet 6700 FT-IR (Thermo Scientific, Waltham, MA, USA) with ATR diamond crystal was used for FTIR spectra collection. The number of scans was set to 32. Raman spectra were measured on a Smart Raman System XploRA™ (Horiba, Kyoto, Japan). A laser of 532 nm (100 mW) was reduced to 1% of the initial intensity. Grating with 600 grooves/mm, acquisition for 10 s, and 10 repetitions were customised. Raman spectra of each sample were measured at 10 different points. The textural properties of the biochar were evaluated via nitrogen physisorption. The nitrogen adsorption–desorption measurements at -196 °C were performed using the Autosorb iQ Station 3 (Quantachrome Instruments, Odelzhausen, Germany). Prior to the nitrogen physisorption measurement, the biochar (0.315 mm particle size) was degassed at 100 °C for 16.9 h under vacuum. The specific surface area, S_{BET} , was calculated according to the Brunauer–Emmett–Teller (BET) theory. The total pore volume was determined from the nitrogen adsorption isotherm at p/p_0 (~ 0.99). The bulk densities of both the feedstock and biochar fraction were determined using a container with a volume of 2 dm³ (79 mm diameter, 470 mm height) and a laboratory-scale XS Balance BL 6001 (XS Instruments, Carpi, Italy) with a maximum permissible error of ± 0.03 g.

3. Results and Discussions

3.1. Parameters of the Producer Gas

The setup of the gasification technology sufficed for the stabilised production of the producer gas parameters, as summarised in Table 1. The producer gas was rich in CH₄ (14.2%_{vol.}), and despite the relatively high content of N₂ (69.8%_{vol.}) due to the usage of air as the oxidising medium, the LHV = 6.33 MJ·m⁻³ was sufficient and very promising, compared to similar studies on fixed bed gasification reactors. On the other hand, the high CH₄ was compensated by much lower contents of CO and H₂, which were only 6.5 and 4.8%_{vol.}, respectively. The presence of CO₂ is a natural consequence of the partial direct combustion of the fuel in the autothermal operation of the reactor. All presented values are defined for STP conditions ($T = 273.15$ K, $p = 101,325$ Pa).

Table 1. Parameters of the sampled producer gas (dry and clean), including standard deviation.

CO [% _{vol.}]	CH ₄ [% _{vol.}]	CO ₂ [% _{vol.}]	H ₂ [% _{vol.}]	O ₂ [% _{vol.}]	N ₂ [% _{vol.}]	LHV [MJ·m ⁻³]	Q [l·min ⁻¹]	Gas Sampling Time [min]
6.5 ± 0.3	14.2 ± 0.1	4.7 ± 0.18	4.8 ± 0.12	0 ± 0.02	69.8 ± 1.28	6.33 ± 0.09	2.2	60

The producer gas parameters can be compared with previous studies, such as the study of Cerone et al. [44], where almond shells were used as the feedstock. The obtained LHV = 6.2 MJ·m⁻³ resulted from the gasification process in the medium-scale device (0.5×2.4 m), with ER = 0.21. However, the gas composition was significantly dissimilar. The CH₄ content was lower (1.7–2.3%_{vol.}), while the H₂ and CO contents were significantly higher (14.3–21.6%_{vol.}; 26.1–30.8%_{vol.}) according to the process conditions, indicating suggestively different management of the gasification process resulting in producer gas appropriate for different utilisations [45]. The differences could be attributed towards differences in the feedstock as well as the design and operation of the gasifier. Cerone et al. [42] performed the gasification process in an updraft gasifier, using almond shells as the feedstock. Moreover, Cerone et al. [42] obtained significant amounts of C_nH_m (ethane and propane alone exceeding 0.5%_{vol.}) and tars (70 g·m⁻³). In the sliding bed reactor developed by the Energy Research Centre in Ostrava and used for the investigation performed within the scope of this work, the gas flows through the bed in a different way, as the bed is relatively flat in comparison to the updraft gasifiers. Therefore, the gas from the

pyrolysis zone is not subject to significant cooling down, as takes place for a gas in an updraft gasifier when flowing through the bed of material [42]. On the other hand, ceramic refractory in the freeboard zone of the sliding bed gasifier allows for a higher residence time of the gas without such a detrimental effect on the gas temperature. It seems plausible to suspect that the methane comes from the thermal cracking ($C_nH_m \rightarrow nC + mH_2/2$) [42] of heavier hydrocarbons and the subsequent methanation of C ($C + 2H_2 \rightarrow CH_4$) [42]. On the other hand, temperatures in the sliding bed gasifier were not favourable for reforming the obtained methane.

Feedstock could also have a significant influence on the results, as Karatas and Akgun [46] achieved CH_4 concentrations of approx. 7% during the gasification of pistachio shells in a laboratory-scale bubbling fluidized bed reactor, with air as a gasification medium, an ER of 0.19, and the gasification temperature maintained at $770^\circ C$ [46]. The study reported that the LHV of the producer gas attained $9.9 MJ \cdot m^{-3}$ (while using steam as a gasification agent) at STP conditions [46]. The experiments with air as a gasifying medium resulted in the LHV of the producer gas accomplishing $5.5 MJ \cdot m^{-3}$ [46]. In a former study of Ćespiva et al. [37], where pure A1 class pellets were used as the input feedstock, the value of LHV reached $4.39 MJ \cdot m^{-3}$ in the same reactor as presented in this study. Also, the ratio between the three mentioned carriers of chemically-bound energy was different ($CH_4/H_2/CO - 5.1/5.8/15.4\%_{vol.}$), probably caused by differences in ER, temperature, and fuel mass flow (efficient use of reactor space). In the study by Cali et al. [47], where pine and eucalyptus wood were gasified in an updraft demo gasifier, the LHVs reached $4.58 MJ \cdot m^{-3}$ in the case of pine and $4.29 MJ \cdot m^{-3}$ in eucalyptus (ER ranging between 0.26–0.33; $CH_4/H_2/CO - 2/12/5-6\%_{vol.}$). A similarly constructed updraft reactor was used by James et al. [48], achieving LHV = $5.59 MJ \cdot m^{-3}$ with ER 0.25. Hosseinzaei et al. [49] performed an investigation on the pyrolysis of pistachio shells at temperatures ranging between $350^\circ C$ and $550^\circ C$ in an investigation of the pyrolysis gas composition. The LHV of the gas was amplified from $4 MJ \cdot m^{-3}$ up to $10 MJ \cdot m^{-3}$ with the increasing temperature of pyrolysis, with methane and other light hydrocarbons contributing significantly to the escalation in the LHV of the pyrolysis gas. Efficiency determination is a tool for the direct comparison of gasification processes regardless of reactor design type, fuel characteristics, and operating conditions. The hot gas efficiency reached 89.6% during the described measurement, while the cold gas efficiency attained its maximum at 73.9%. Both values were attained with respect to an amount of producer gas flow equal to $15.3 m^3 \cdot h^{-1}$. The average gas production rate was then around $2.1 m^3 \cdot kg^{-1}$.

3.2. Characterization of Carbonaceous Material

The separated carbonaceous material (gasified pistachio shells) derived from the gasification process was solely used for analysis in accordance with the aforementioned procedure. A photographic image of the gasified pistachio shells is presented in Figure 2. Table 2 depicts the results of the ultimate and proximate analyses, where data from the analyses of the raw material are included for comparison. The bulk density of raw pistachio shells was estimated to be $286.9 kg \cdot m^{-3}$, while the bulk density of gasified pistachio shells was assessed to be $226.4 kg \cdot m^{-3}$.



Figure 2. A photo of gasified pistachio shells.

Table 2. Raw and gasified PS characteristics (wherever not marked, values are on a dry basis; ar—values on an as-received basis; oxygen content calculated by difference; n.d.—not determined; SRF—solid recovered fuel).

	C [%wt]	H [%wt]	N [%wt]	S [%wt]	O [%wt]	Moisture Content [%wt]	Ash [%wt]	LHV [MJ·kg ⁻¹]	pH [–]	Bulk Density [kg·m ⁻³]
Raw pistachio shells ^{ar} (this study)	43.85 ± 2.20 ^{ar}	5.38 ± 0.19 ^{ar}	<0.20 ± 0.10 ^{ar}	<0.02 ± 0.10 ^{ar}	40.94	8.64 ± 0.24 ^{ar}	0.97 ± 0.56 ^{ar}	16.00 ± 2.40 ^{ar}	4.70 ± 0.01 ^{ar}	286.90 ± 1.20 ^{ar}
Gasified pistachio shells (this study)	62.08 ± 2.50 ^{ar}	4.71 ± 0.17 ^{ar}	0.21 ± 0.10 ^{ar}	0.02 ± 0.10 ^{ar}	27.69	2.96 ± 0.11 ^{ar}	2.33 ± 0.78 ^{ar}	22.51 ± 2.40 ^{ar}	9.52 ± 0.01 ^{ar}	226.40 ± 1.30 ^{ar}
Gasified olive pomace pellets ^d [41]	69.5 ± 0.20 ^{ar}	0.80 ± 0.10 ^{ar}	1.54 ± 0.05 ^{ar}	0.34 ± 0.03 ^{ar}	5.90	10.50 ± 0.10 ^{ar}	21.90 ± 0.10 ^{ar}	n.d.	n.d.	363 ^{ar}
Gasified softwood pellets ^d [23]	81.1 ^{ar}	2.6 ^{ar}	0.2 ^{ar}	0.0 ^{ar}	10.8 ^{ar}	4.1 ^{ar}	1.2	n.d.	n.d.	333 – 351 ^{* ar}
Gasified, steam-activated, softwood pellets ^{ar} [23]	93.4 ^{ar}	0.8 ^{ar}	0.5 ^{ar}	0.0 ^{ar}	1.3 ^{ar}	2.0 ^{ar}	2.0	n.d.	n.d.	284 – 308 ^{* ar}
Gasified SRF ^{ar} [23]	73.7 ^{ar}	1.4 ^{ar}	0.9 ^{ar}	0.1 ^{ar}	5.3 ^{ar}	7.7 ^{ar}	11.0	n.d.	n.d.	250 – 272 ^{* ar}
Gasified, steam-activated, SRF ^{ar} [23]	80.0	0.7	0.8	0.1	1.3	2.7 ^{ar}	13.9	n.d.	n.d.	217 – 238 ^{* ar}
Pistachio shells torrefied at 200 °C ^d [50]	48.1	5.38	46.3 ^{**}	<0.01	46.3 ^{**}	7.32 ^{ar}	0.19	n.d.	n.d.	n.d.
Pistachio shells torrefied at 300 °C ^d [50]	62.3	3.85	32.9 ^{**}	<0.01	32.9 ^{**}	5.78 ^{ar}	0.90	n.d.	n.d.	n.d.
Pistachio shells after pyrolysis at 400 °C ^d [50]	76.2	3.5	19.3 ^{**}	<0.01	19.3 ^{**}	3.73 ^{ar}	0.96	n.d.	n.d.	n.d.
Pistachio shells after pyrolysis at 600 °C ^d [50]	87.2	2.23	9.5 ^{**}	<0.01	9.5 ^{**}	1.82 ^{ar}	1.09	n.d.	n.d.	n.d.
Pistachio shells after pyrolysis at 850 °C ^d [50]	88.0	1.18	9.5 ^{**}	<0.01	9.5 ^{**}	0.44 ^{ar}	1.37	n.d.	n.d.	n.d.
Bamboo biochar ^d [51]	77.63	2.81	1.07	0.17	18.32	4.68 ^{ar}	3.90	n.d.	10.1	n.d.

Note: The oxygen content was calculated; ar—as-received (wet) basis; d—dry basis; *—depending on the particle size; **—reported as O + N; n.d.—not determined.

The pH values of the raw and gasified pistachio shells were determined to be 4.7 and 9.52 on the pH scale, respectively. The upsurge in pH value could have been caused by the transformation of inorganic materials during the gasification process, which might have influenced the pH of the output products. For instance, the release of acidic compounds was capable of increasing the pH of solid residues while reducing the pH of producer gas [52].

Nowicki et al. [53] described the acid–base properties of the activated carbon produced through the pyrolysis technique and the consequent activation of the pistachio shells. The acidity was primarily dependent on the process of activation. Char activated by H_3PO_4 had a pH of 2.22, while char activated by CO_2 had a pH of 10.6 (non-activated char was not measured), although in this present study, it was also alkaline. El-Bassi et al. [54] described the acid–base properties of the biochar produced from exhausted grapes as a function of the pyrolysis temperature (300 and 500 °C). It was determined that with increasing temperature, the pH also increased from 7.2 to 9.9, which was in agreement with other published works. A similar trend was observed by Komnitsas et al. [55] during the pyrolysis of pistachio shells, with a resulting value of pH fluctuating between 4.68 and 8.81 in the temperature range of 250–650 °C.

The variability in the pH value was observed by other authors dealing primarily with soil amendment applications. The biochars prepared from corn straw and oak sawdust by pyrolysis were used as a soil amendment material in the study of Li et al. [56], with the resulting pH ranging between 6.63 and 8.50. Their application into the soil had a limited effect on its properties. However, calcium modification after the treatment significantly increased the influence of their application. A study by Shaoqing et al. [57] described the properties of pyrolytically prepared biochars (at 500 °C for 2 h) from halophyte *Salicornia europaea* and glycophyte *Zea mays*, with pH values reaching 10.39 ± 1.37 and 9.09 ± 1.32 .

Moreover, the advantage of the described material usage was the carbon mass fraction, which optimistically impacted the soil properties from the carbon sequestration and water retention points of view [58]. Nonetheless, a detailed analysis of the trace elements should be performed before the application of biochar as a fertilizing substitute to avoid the hazard of contamination by persistent and environmentally harmful substances. A detailed analysis of the pistachio shell biochar ash is tabulated in Table 3.

Table 3. Detailed substance analysis of the pistachio shell ash.

Al_2O_3 [%wt]	CaO [%wt]	Cl [%wt]	Cr_2O_3 [%wt]	CuO [%wt]	Fe_2O_3 [%wt]	K_2O [%wt]
0.58	2.40	32.50	0.0003	0.0005	0.05	7.44
MgO [%wt]	MnO [%wt]	Na_2O [%wt]	NiO [%wt]	P_2O_5 [%wt]	PbO [%wt]	SiO_2 [%wt]
0.15	0.0009	40.08	0.0006	0.94	0.0014	0.34
SO_3 [%wt]	SrO [%wt]	TiO_2 [%wt]	ZnO [%wt]			
1.13	0.0017	0.0011	0.0014			

Note: SUM = 85.62%_{wt}, ash by TGA = 85.73%_{wt}, weight loss by annealing in TGA (950 °C) = 14.27%_{wt}, total SUM 99.89%_{wt}. Compounds with a mass fraction below the limit of detection (limit of detection): Ag (0.0002%_{wt}), As (0.000007%_{wt}), Ba (0.00002%_{wt}), Cd (0.00002%_{wt}), Cr (0.000001%_{wt}), Na (0.002%_{wt}), Se (0.000001%_{wt}), V (0.00002%_{wt}).

In comparison with biochar originating from different feedstocks (kenaf stems [59] and rice husk [60]) treated by pyrolysis, the most significant differences were in Cl and Na_2O mass fractions. High mass fractions of these two compounds may be caused by pretreatment of the pistachio before selling—the addition of $NaCl$ for their flavouring. However, the combination of Na and Cl might positively affect the soil salinity and, consequently, influence the yield of some crops, such as *Raphanus sativus* [61].

It should not be overlooked that the contents of heavy metals and polycyclic aromatic hydrocarbons (PAH) are limited by national and international legislation documents [41,62,63]. One of the most complex legislation documents aimed at soil quality is the Government Decree on the Assessment of Soil Contamination and Remediation Needs of Finland [64], including the limit values for antimony (Sb), arsenic (As), mercury (Hg), cadmium (Cd),

cobalt (Co), chrome (Cr), copper (Cu), lead (Pb), nickel (Ni), zinc (Zn), and vanadium (V). Similarly, obtaining certification of biochar (European Biochar Certificate) requires, among others, the determination of the content of heavy metals and PAH [65]. Another aspect that is worth considering is the fact that the biochar prepared using thermochemical pistachio shells has been proven to be an effective option for heavy metal adsorbing [55]. However, the suitability of using biochar as an adsorbent is determined by its physicochemical properties, including physical parameters describing pores (porosity, pore size distribution, surface area, volume) as well as the presence of particular functional groups at the particles' surface, which vary according to the method of preparation and subsequent activation.

The presence of different functional groups at the surface of the produced biochars could be determined based on the obtained FTIR spectra presented in Figure 3. The FTIR spectra of ground, non-gasified pistachio shells corresponded to spectra reported in the literature [66]. Infrared spectroscopy revealed the occurrence of alkane (C–C), alkene (C=C), hydroxy (–OH), alkyl (C–H), ester (C=O), alkoxy (C–O), and ether (C–O–C) functional groups of untreated and gasified pistachio shells. The most intensive bands in both spectra at 3336 – 3365 cm^{-1} were connected to –OH bonds. This broadband was assigned to O–H stretching of H_2O , the intensity of which decreased with drying [35]. Bands in lower wavenumbers were connected to the different stretching and deformation vibrations of cellulose, hemicellulose, and lignin. Although both samples contained bands connected to similar compounds, several differences did persist. Variances between untreated pistachio shells and gasified pistachio shells were prominently observable. The bands in the region of 1700 – 500 cm^{-1} were broader, and were connected to a more amorphous structure in gasified pistachio shells. Correspondingly, the band at 1731 cm^{-1} (C=O) disappeared (due to the decomposition of the lignin), several bands lost their intensities (e.g., 1034 cm^{-1} in pistachio shells), and their positions were shifted (e.g., 1020 cm^{-1} in gasified pistachio shells), which is again connected to the decomposition of the cellulose/hemicellulose/lignin and other organic compounds due to thermochemical treatment, as previously described in [55]. Band positions are summarised in Tables 4 and 5.

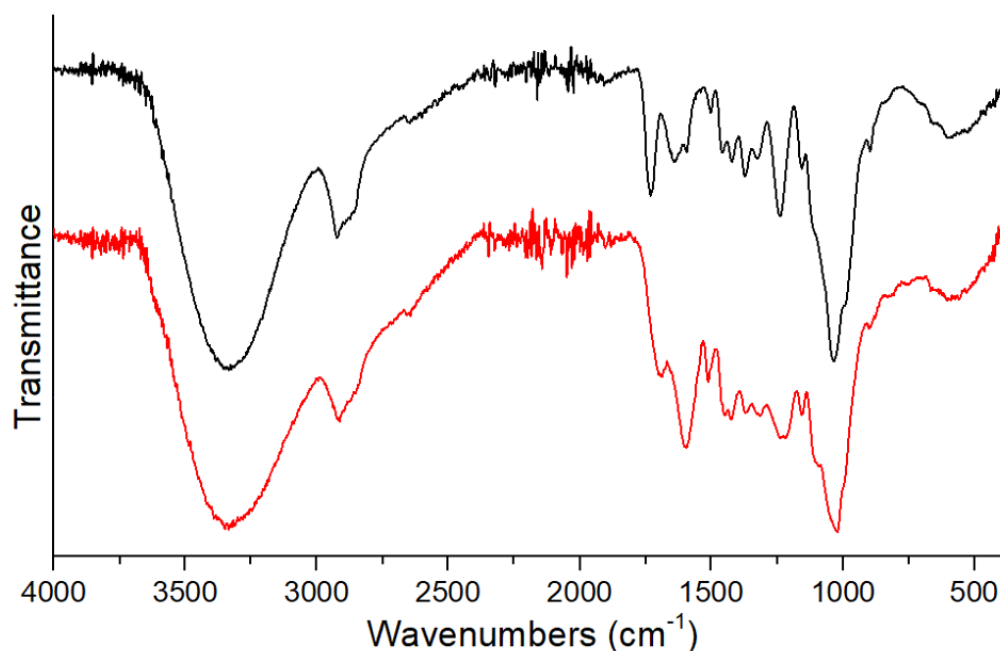


Figure 3. FTIR spectra of untreated (black) and gasified (red) pistachio shells.

FTIR spectra of untreated pistachio shells and activated carbons from pistachio shells were described previously, e.g., by da Silva et al. [67], who studied the combustion of pistachio shells and exhibited similar functional groups of untreated pistachio shells to the presented material. Other groups, such as alkyne stretching vibration of $\text{C}\equiv\text{C}$ (2139 cm^{-1}),

carboxylic acid groups C–O–H (1427 cm^{-1}), and =C–H bending in alkynes (604 cm^{-1}) were found in untreated pistachio shells. Açıkalın et al. [66] studied the pyrolysis of pistachio shells and presented the difference between raw pistachio shells and solid products obtained at different pyrolysis temperatures. Some of the functional groups present in the pistachio shells were removed partially or totally from the structure with increasing temperature. At the same time, a decrease in the aliphaticity and an upsurge in the aromaticity of the solid product were observed. With higher temperatures (500 °C and higher), the decrease in aromaticity of the solid product was indicative.

Table 4. Band assignments of FTIR spectra for raw and gasified pistachio shells.

Raw PS [cm^{-1}]	Gasified PS [cm^{-1}]	Band Assignment	Ref.
3335	3336	O–H stretching vibration in hydroxyl groups	[55,66,68]
2922, 2857	2914, 2853	aliphatic CH asymmetric and symmetric stretching vibration	[66,68]
1731		C=O stretching vibration in carbonyl or carboxylic bonds	[55,66,68]
	1691	conjunction of the carbonyl group with the aromatic ring	[66]
1637, 1594	1594	aromatic C=O ring or C=C aromatic in lignin, skeletal vibration	[55,66]
1503, 1458, 1421	1513, 1449, 1425	aromatic C=O and C=C ring stretching	[55,66]
1373	1371	CH deformation vibration in alkanes and alkyl groups	[55,66]
1238	1237	C=C stretching	[55]
1156, 1034	1157, 1020	aliphatic ether, alcohol C–O or aromatic stretching, O–H deformation, b-glycosidic bond in cellulose and hemicellulose	[55,66]
900–500	900–500	CH wagging vibrations	[55,66]

Table 5. Band assignments of FTIR spectra for hemicellulose, cellulose, and lignin in raw and gasified pistachio shells.

	Raw Pistachio Shells [cm^{-1}]	Gasified Pistachio Shells [cm^{-1}]	Ref.
Hemicellulose	1458, 1238, 1156, 1034	1449, 1237, 1157, 1020	[68]
Cellulose	1421, 1373, 1034	1425, 1371, 1020	[68]
Lignin	1594, 1503	1594, 1511	[68]

In the case of gasified pistachio shells, the intensities of the D and G bands (characteristic bands of carbonaceous materials) were relatively high at only a few points to be distinguishable in the fluorescence background. This outcome served as a clear suggestion that the remaining compounds in the sample could have been the source of the fluorescence. Likewise, at certain points, bands were measured in the lower wave numbers, which could be connected to the presence of TiO_2 in the rutile or anatase phase (according to the spectral library). Due to the high fluorescence, the ratio between D and G bands was complicated to determine. FTIR and Raman spectra of raw pistachio shells and their activated carbon were described in the study of Foroushani et al. [69].

Specific surface area, pore volume, and pore diameter are considered as important values for various possible applications of the material, including its use as a feedstock for the production of activated carbon. The study of Niksiar and Nasernejad [70] was aimed at optimising the production process of activated carbon with the highest possible specific

surface area, using pyrolysis in a spouted bed reactor. The chars produced by pyrolysis reached a specific surface area of $430 \text{ m}^2 \cdot \text{g}^{-1}$ [70], while after the steam activation (under temperature $750\text{--}850 \text{ }^\circ\text{C}$), they achieved a specific surface area that was increased up to $2596 \text{ m}^2 \cdot \text{g}^{-1}$ [70].

Wu et al. [71] focused their study on the preparation of sorbents from pistachio shells, while the carbonaceous process consisted of calcination ($550 \text{ }^\circ\text{C}$) of the input material in a ceramic oven. Two strategies of char activation were employed, namely, steam activation and KOH activation. After the processes, the specific surfaces reached $1009 \text{ m}^2 \cdot \text{g}^{-1}$ (steam activation) and $1096 \text{ m}^2 \cdot \text{g}^{-1}$ (KOH activation). The specific surface areas of char without activation were not listed. The pore volume for both techniques ranged between 0.61 and $0.67 \text{ cm}^3 \cdot \text{g}^{-1}$, and the pore diameter ranged between 2.2 and 2.6 nm .

The second study by Wu et al. [72] was also focussed strictly on laboratory preparation of adsorbents from pistachio shells following the aforementioned techniques, with an annealing temperature of $450 \text{ }^\circ\text{C}$, under different KOH/char ratios. The best KOH/char ratio from the highest accomplished specific surface area point of view proved to be ratio 3, in which it achieved a specific surface area of $1,687 \text{ m}^2 \cdot \text{g}^{-1}$ (pore diameter: 2.6 nm , pore volume: $1.08 \text{ cm}^3 \cdot \text{g}^{-1}$). A. C. Lua and Yang [73] performed pyrolysis of pistachio shells, along with subsequent CO_2 activation. The resulting specific surface area ranged between 333 and $778 \text{ m}^2 \cdot \text{g}^{-1}$ according to the pyrolysis temperature. The pore volume ranged, according to the same parameter, between 0.078 and 0.466 . The highest specific surface and pore volume were reached at a pyrolysis temperature of $500 \text{ }^\circ\text{C}$ and a hold time of 2 h . The quality of the producer gas was not determined. The same temperature proved to be the best in the case of vacuum pyrolysis during the study of A. C. Lua and Yang [34], where a higher specific surface ($896 \text{ m}^2 \cdot \text{g}^{-1}$) and pore volume ($0.237 \text{ cm}^3 \cdot \text{g}^{-1}$) were reported. The average pore diameter under the mentioned conditions was 2.38 nm . In the study of Faramarzi et al. [36], the crushed and sieved pistachio shells underwent a pyrolysis process in the laboratory-scale tubular reactor. A pyrolysis temperature of $600 \text{ }^\circ\text{C}$, a heating rate of $20 \text{ }^\circ\text{C} \cdot \text{min}^{-1}$, a 1 h hold time, and an N_2 flow rate of $100 \text{ ml} \cdot \text{min}^{-1}$ were the best conditions to produce char with a specific surface area of $350 \text{ m}^2 \cdot \text{g}^{-1}$, which was approximately seven times higher than the results obtained in this study. The activation process for increasing the specific surface area was only mathematically modelled. Foo and Hameed [74] used a laboratory pyrolysis reactor heated at $700 \text{ }^\circ\text{C}$ under a pure nitrogen atmosphere. Activation of the char by KOH occurred under a ratio of $1:1.75$ (char:KOH) in a modified microwave oven. The specific surface area was listed for non-activated ($115 \text{ m}^2 \cdot \text{g}^{-1}$) and activated pistachio shells ($700 \text{ m}^2 \cdot \text{g}^{-1}$). The total pore volume also significantly differed between the non-activated char ($0.069 \text{ cm}^3 \cdot \text{g}^{-1}$) and activated char ($0.375 \text{ cm}^3 \cdot \text{g}^{-1}$). The composition of the producer gas was not provided in this study. The biochar made via the pyrolysis of bamboo was presented in the study of Deng et al. [51], where similar surface area and pore size ($S_{\text{bet}} = 46.93 \text{ m}^2 \cdot \text{g}^{-1}$, $V_p = 0.04 \text{ cm}^3 \cdot \text{g}^{-1}$) were accomplished, while the biochar application proved to be an efficient method for limiting the translocation of Cr into aboveground plant parts, which enhanced the antioxidant activities and reduced the harmful effects.

Considering the studies describing the similar thermal treatment of biomass-based material as in the presented study, the resulting values can be compared with the research study of Čespiva et al. [23], where the certified A1 pellet was gasified in the same reactor as that mentioned in this study. The specific surface of non-activated char ranged between 36.1 and $37.7 \text{ m}^2 \cdot \text{g}^{-1}$ (according to the fraction granulometry), its pore diameter ranged between 3.01 and 3.5 nm , and its pore volume was $0.03 \text{ cm}^3 \cdot \text{g}^{-1}$, which are very analogous values to the newly presented ones. All three mentioned parameters increased after the steam activation: the specific area ranged between 661 and $737.2 \text{ m}^2 \cdot \text{g}^{-1}$, the pore diameter ranged between 3.33 and 3.6 nm , and the pore volume ranged between 0.19 and $0.33 \text{ cm}^3 \cdot \text{g}^{-1}$. The significant increase in the mentioned parameters enabled a remarkable capture of mercury from flue gas produced during coal combustion. The results obtained

from the nitrogen physisorption of the gasified pistachio shells are tabularized in Table 6, along with a comparison of the literature data.

Table 6. Textural physisorption—results of this study in comparison to other works.

Sample	Specific Surface Area [$\text{m}^2 \cdot \text{g}^{-1}$]	Average Pore Diameter [nm]	Total Pore Volume [$\text{cm}^3 \cdot \text{g}^{-1}$]	Reference
Pistachio shells after gasification in cross-updraft hybrid gasifier	50.89	3.55	0.035	This study
Pistachio shells after vacuum pyrolysis at 350 °C and subsequent CO ₂ activation at 900 °C	611	2.57	0.393	[34]
Pistachio shells after vacuum pyrolysis at 400 °C and subsequent CO ₂ activation at 900 °C	874	2.33	0.509	[34]
Pistachio shells after vacuum pyrolysis at 500 °C and subsequent CO ₂ activation at 900 °C	896	2.38	0.532	[34]
Pistachio shells after vacuum pyrolysis at 600 °C and subsequent CO ₂ activation at 900 °C	645	2.63	0.424	[34]
Pistachio shells after vacuum pyrolysis at 700 °C and subsequent CO ₂ activation at 900 °C	690	2.63	0.454	[34]
Pistachio shells after vacuum pyrolysis at 800 °C and subsequent CO ₂ activation at 900 °C	724	2.51	0.454	[34]
Pistachio shells after vacuum pyrolysis at 900 °C and subsequent CO ₂ activation at 900 °C	724	2.07	0.374	[34]
Pistachio shells after vacuum pyrolysis at 1000 °C and subsequent CO ₂ activation at 900 °C	418	1.97	0.206	[34]
Pistachio shells after pyrolysis at 700 °C	115.5	2.339	0.069	[74]
Pistachio shells after pyrolysis at 700 °C and subsequent KOH activation using microwaves (7 min)	700.5	2.144	0.375	[74]

As can be understood from Table 6, other processes, such as pyrolysis, are proficient at producing char with a higher specific surface area, lower average pore diameter, and an advanced total pore volume. The pyrolysis of pistachio shells at 700 °C, performed by Foo and Hameed [74], resulted in a specific surface area that was more than two times higher than the char produced within the scope of this study. However, the literature studies shown in Table 6 clearly indicated the fact that activation was indeed essential after pyrolysis in order to produce activated carbon with a surface area sufficient to make such activated carbon beneficial. In pyrolysis, the heat supply for the process is a crucial parameter to be solved, along with the energy requirements needed to create vacuum conditions, implying additional consumption of energy. On the other hand, gasification, performed within the scope of this study, was autothermal. Therefore, no external energy source was required apart from the fuel for startup. Moreover, gasification produced combustible gas, which can be used for the generation of electricity and heat in a CHP unit. Furthermore, heat recovered by the CHP unit could be used to generate the steam necessary for activation. Thus, the advantage of gasification lies in the possibility of supplying the needs of the installation, along with the production of surplus energy, which would be the key for a self-sufficient polygeneration installation producing electricity, heat, activated carbon, and biochar (solid residues from wood pellets). Further work is recommended in order to quantify the benefits of using gasification as the first step before activation of the solid residues from the gasification process, including the comprehensive mass and energy balances of such an installation. Consistently, sustainability analysis appears to be important in context of such novel technologies in bioenergy systems [75]. The results presented in this work provide a good starting point for such an extensive analysis.

4. Conclusions and Future Perspectives

The pistachio shells proved to be an appropriate material for co-gasification with wood pellets in a pilot-scale cross/updraft type reactor, resulting in technologically applicable

producer gas and valuable biochar. The gasification process caused a change in many chemical properties of the pistachio shells, which significantly facilitated its applicability in various industries. Analysis of the pistachio shells' biochar unveiled noteworthy transformations. The obtained biochar exhibited a high LHV = 22.51 MJ·kg⁻¹, alkaline pH (9.52), and altered chemical composition. The pH shift from 4.7 in raw pistachio shells to 9.52 in the gasified material suggests transformations in inorganic materials during gasification, impacting the product's pH.

Co-gasification, performed within the scope of this study, was autothermal. Thus, no external energy source was needed aside from the fuel needed for startup. The process produced combustible gas with an LHV of 6.53 MJ·m⁻³, which could be used for the generation of electricity and heat in a CHP unit.

These aforementioned outcomes may be especially interesting for pistachio nut producers, mostly situated in locations where intermittent but intense sources of renewable energy, namely, solar energy through direct photovoltaics or photothermal harvest principle, are available. The intermittence would not be harmful in this case, as the accumulated material could be utilised solely in inappropriate energy supply conditions.

Further in-depth research analyses, with detailed mass and energy balances of such novel installations, as well as comprehensive analyses of economic feasibility and environmental impact, are recommended for quantification of the benefits of using gasification as the first step before activation of the solid residues from the gasification process. Moreover, future research endeavours should determine whether the char from the gasification process could be applied to soil as biochar, which would require a comprehensive investigation of the deposition of PAH on the surface of biochar during gasification in sliding bed conditions.

Author Contributions: Conceptualization, J.R., J.Č. and L.N.; methodology, J.R. and J.Č.; validation, J.R. and J.Č.; formal analysis, J.R., J.Č. and L.N.; investigation, J.R., J.Č. and L.N.; resources, L.K. and M.D.; data curation, J.R., J.Č., K.S.-S. and L.N.; writing—original draft preparation, J.R., J.Č. and L.N.; writing—review and editing, J.R., J.Č., W.-M.Y. and S.T.; supervision, O.M.; project administration, J.R.; funding acquisition, J.R. All authors have read and agreed to the published version of the manuscript.

Funding: This work was co-financed by the Recovery and Resilience Facility within the National Centre for Energy II, reg. no. TN02000025. It was also financially supported by the European Union under the REFRESH – Research Excellence For Region Sustainability and High-tech Industries project No. CZ.10.03.01/00/22_003/0000048 via the Operational Programme Just Transition.

Institutional Review Board Statement: Not applicable.

Informed Consent Statement: Not applicable.

Data Availability Statement: Data are available upon personal request to the correspondence author.

Conflicts of Interest: The authors declare no conflicts of interest.

Nomenclature

ATR	attenuated total reflectance
BECCS	bioenergy with carbon capture and storage
BET	Brunauer–Emmett–Teller
CCU	carbon capture and use
CCS	carbon capture and storage
CGE	cold gas efficiency
CHP	combined heat and power
ECD	electrochemical detector
ER	equivalence ratio
FTIR	Fourier transform infrared
HHV	higher heating value
HGE	hot gas efficiency
LHV	lower heating value

NDIR	non-dispersive infrared
PAH	polycyclic aromatic hydrocarbons
STP	standard temperature and pressure
TCD	thermal conductivity detector
TGA	thermogravimetric analysis
XRF	X-ray fluorescence

References

- Bury, M.; Dziok, T.; Borovec, K.; Burmistrz, P. Influence of RDF Composition on Mercury Release during Thermal Pretreatment. *Energies* **2023**, *16*, 772. [\[CrossRef\]](#)
- Mehmood, A.; Tahir, M.W.; Saeed, M.A.; Arshad, M.Y.; Hussain, H.; Mularski, J.; Niedzwiecki, L. Optimization of Gasifying Agents in 3D Downdraft Gasification for Enhanced Gas Composition, Combustion, and CO₂ Utilization. *Fire* **2023**, *6*, 361. [\[CrossRef\]](#)
- Ziółkowski, P.; Badur, J.; Pawlak-Kruczek, H.; Stasiak, K.; Amiri, M.; Niedzwiecki, L.; Krochmalny, K.; Mularski, J.; Madejski, P.; Mikielwicz, D. Mathematical modelling of gasification process of sewage sludge in reactor of negative CO₂ emission power plant. *Energy* **2022**, *244*, 122601. [\[CrossRef\]](#)
- Yang, Y.; Shahbeik, H.; Shafizadeh, A.; Rafiee, S.; Hafezi, A.; Du, X.; Pan, J.; Tabatabaei, M.; Aghbashlo, M. Predicting municipal solid waste gasification using machine learning: A step toward sustainable regional planning. *Energy* **2023**, *278*, 127881. [\[CrossRef\]](#)
- Li, H.; Chen, J.; Zhang, W.; Zhan, H.; He, C.; Yang, Z.; Peng, H.; Leng, L. Machine-learning-aided thermochemical treatment of biomass: A review. *Biofuel Res. J.* **2023**, *10*, 1786–1809. [\[CrossRef\]](#)
- Kolios, G.; Frauhammer, J.; Eigenberger, G. Autothermal fixed-bed reactor concepts. *Chem. Eng. Sci.* **2000**, *55*, 5945–5967. [\[CrossRef\]](#)
- Kuba, M.; Hofbauer, H. Experimental parametric study on product gas and tar composition in dual fluid bed gasification of woody biomass. *Biomass Bioenergy* **2018**, *115*, 35–44. [\[CrossRef\]](#)
- Zhou, J.; Chen, Q.; Zhao, H.; Cao, X.; Mei, Q.; Luo, Z.; Cen, K. Biomass-oxygen gasification in a high-temperature entrained-flow gasifier. *Biotechnol. Adv.* **2009**, *27*, 606–611. [\[CrossRef\]](#)
- Sandeep, K.; Dasappa, S. Oxy-steam gasification of biomass for hydrogen rich syngas production using downdraft reactor configuration. *Int. J. Energy Res.* **2014**, *38*, 174–188. [\[CrossRef\]](#)
- Sun, Y.; Zhang, Z.; Liu, L.; Wang, X. Two-stage high temperature sludge gasification using the waste heat from hot blast furnace slags. *Bioresour. Technol.* **2015**, *198*, 364–371. [\[CrossRef\]](#)
- Sun, Y.; Liu, Q.; Wang, H.; Zhang, Z.; Wang, X. Role of steel slags on biomass/carbon dioxide gasification integrated with recovery of high temperature heat. *Bioresour. Technol.* **2017**, *223*, 1–9. [\[CrossRef\]](#)
- Duan, W.; Yu, Q.; Liu, J.; Wu, T.; Yang, F.; Qin, Q. Experimental and kinetic study of steam gasification of low-rank coal in molten blast furnace slag. *Energy* **2016**, *111*, 859–868. [\[CrossRef\]](#)
- Vakalis, S.; Sotiropoulos, A.; Moustakas, K.; Malamis, D.; Baratieri, M. Utilisation of biomass gasification by-products for onsite energy production. *Waste Manag. Res.* **2016**, *34*, 564–571. [\[CrossRef\]](#)
- Alcazar-Ruiz, A.; Ortiz, M.L.; Dorado, F.; Sanchez-Silva, L. Gasification versus fast pyrolysis bio-oil production: A life cycle assessment. *J. Clean. Prod.* **2022**, *336*, 130373. [\[CrossRef\]](#)
- Tijmensen, M.J.A.; Faaij, A.P.C.; Hamelinck, C.N.; van Hardeveld, M.R.M. Exploration of the possibilities for production of Fischer Tropsch liquids and power via biomass gasification. *Biomass Bioenergy* **2002**, *23*, 129–152. [\[CrossRef\]](#)
- Zhang, Q.; Kang, J.; Wang, Y. Development of Novel Catalysts for Fischer-Tropsch Synthesis: Tuning the Product Selectivity. *ChemCatChem* **2010**, *2*, 1030–1058. [\[CrossRef\]](#)
- Ertesvåg, I.S.; Madejski, P.; Ziółkowski, P.; Mikielwicz, D. Exergy analysis of a negative CO₂ emission gas power plant based on water oxy-combustion of syngas from sewage sludge gasification and CCS. *Energy* **2023**, *278*, 127690. [\[CrossRef\]](#)
- Luo, S.; Fu, J.; Zhou, Y.; Yi, C. The production of hydrogen-rich gas by catalytic pyrolysis of biomass using waste heat from blast-furnace slag. *Renew. Energy* **2017**, *101*, 1030–1036. [\[CrossRef\]](#)
- Yao, X.; Liu, Y.; Yu, Q.; Wang, S. Energy consumption of two-stage system of biomass pyrolysis and bio-oil reforming to recover waste heat from granulated BF slag. *Energy* **2023**, *273*, 127204. [\[CrossRef\]](#)
- Yao, X.; Yu, Q.; Han, Z.; Xie, H.; Duan, W.; Qin, Q. Kinetics of CO₂ gasification of biomass char in granulated blast furnace slag. *Int. J. Hydrog. Energy* **2018**, *43*, 12002–12012. [\[CrossRef\]](#)
- Manga, M.; Aragón-Briceño, C.; Boutikos, P.; Semiyaga, S.; Olatinjo, O.; Muoghalu, C.C. Biochar and Its Potential Application for the Improvement of the Anaerobic Digestion Process: A Critical Review. *Energies* **2023**, *16*, 4051. [\[CrossRef\]](#)
- Hansen, V.; Müller-Stöver, D.; Ahrenfeldt, J.; Holm, J.K.; Henriksen, U.B.; Hauggaard-Nielsen, H. Gasification biochar as a valuable by-product for carbon sequestration and soil amendment. *Biomass Bioenergy* **2015**, *72*, 300–308. [\[CrossRef\]](#)
- Čespiva, J.; Jadlovec, M.; Výtisk, J.; Serenčíšová, J.; Tadeáš, O.; Honus, S. Softwood and solid recovered fuel gasification residual chars as sorbents for flue gas mercury capture. *Environ. Technol. Innov.* **2023**, *29*, 102970. [\[CrossRef\]](#)
- Zelenková, G.; Zelenka, T.; Slovák, V. Thermoporometry of porous carbon: The effect of the carbon surface chemistry on the thickness of non-freezable pore water layer (delta layer). *Microporous Mesoporous Mater.* **2021**, *326*, 111358. [\[CrossRef\]](#)

25. Jeswani, H.K.; Gujba, H.; Brown, N.W.; Roberts, E.P.L.; Azapagic, A. Removal of organic compounds from water: Life cycle environmental impacts and economic costs of the Arvia process compared to granulated activated carbon. *J. Clean. Prod.* **2015**, *89*, 203–213. [CrossRef]
26. Mlonka-Mędrala, A.; Hasan, T.; Kalawa, W.; Sowa, M.; Sztokler, K.; Pinto, M.L.; Mika, L. Possibilities of Using Zeolites Synthesized from Fly Ash in Adsorption Chillers. *Energies* **2022**, *15*, 7444. [CrossRef]
27. Subrahmanyam, K.S.; Spanopoulos, I.; Chun, J.; Riley, B.J.; Thallapally, P.K.; Trikalitis, P.N.; Kanatzidis, M.G. Chalcogenide aerogels as sorbents for noble gases (Xe, Kr). *ACS Appl. Mater. Interfaces* **2017**, *9*, 33389–33394. [CrossRef]
28. Statista. Production of Pistachios Worldwide from 2007/2008 to 2020/2021. Available online: <https://www.statista.com/statistics/933073/pistachio-global-production/> (accessed on 8 February 2024).
29. Ryšavý, J.; Serenčíšová, J.; Horák, J.; Ochodek, T. The co-combustion of pellets with pistachio shells in residential units additionally equipped by Pt-based catalyst. *Biomass Convers. Biorefinery* **2023**, *13*, 16511–16527. [CrossRef]
30. Palma, A.; Gallucci, F.; Papandrea, S.; Carnevale, M.; Paris, E.; Vincenti, B.; Salerno, M.; Di Stefano, V.; Proto, A.R. Experimental Study of the Combustion of and Emissions from Olive and Citrus Pellets in a Small Boiler. *Fire* **2023**, *6*, 288. [CrossRef]
31. Ryšavý, J.; Horák, J.; Kuboňová, L.; Jaroch, M.; Hopan, F.; Krpec, K.; Kubesa, P. Beech leaves briquettes as fuel for a home combustion unit. *WIT Trans. Ecol. Environ.* **2020**, *246*, 75–85. [CrossRef]
32. Ryšavý, J.; Horák, J.; Kuboňová, L.; Jaroch, M.; Hopan, F.; Krpec, K.; Kubesa, P. Beech leaves briquettes' and standard briquettes' combustion: Comparison of flue gas composition. *Int. J. Energy Prod. Manag.* **2021**, *6*, 32–44. [CrossRef]
33. Hu, C.-C.; Wang, C.-C.; Wu, F.-C.; Tseng, R.-L. Characterization of pistachio shell-derived carbons activated by a combination of KOH and CO₂ for electric double-layer capacitors. *Electrochim. Acta* **2007**, *52*, 2498–2505. [CrossRef]
34. Lua, A.C.; Yang, T. Effects of vacuum pyrolysis conditions on the characteristics of activated carbons derived from pistachio-nut shells. *J. Colloid Interface Sci.* **2004**, *276*, 364–372. [CrossRef]
35. Vijayalakshmi, P.; Bala, V.S.S.; Thiruvengadaravi, K.V.; Panneerselvam, P.; Palanichamy, M.; Sivanesan, S. Removal of acid violet 17 from aqueous solutions by adsorption onto activated carbon prepared from pistachio nut shell. *Sep. Sci. Technol.* **2011**, *46*, 155–163. [CrossRef]
36. Faramarzi, A.H.; Kaghazchi, T.; Ebrahim, H.A.; Ebrahimi, A.A. Experimental investigation and mathematical modeling of physical activated carbon preparation from pistachio shell. *J. Anal. Appl. Pyrolysis* **2015**, *114*, 143–154. [CrossRef]
37. Čespiva, J.; Niedzwiecki, L.; Vereš, J.; Skřínský, J.; Wnukowski, M.; Borovec, K.; Ochodek, T. Evaluation of the performance of the cross/updraft type gasification technology with the sliding bed over a circular grate. *Biomass Bioenergy* **2022**, *167*, 106639. [CrossRef]
38. Čespiva, J.; Niedzwiecki, L.; Wnukowski, M.; Krochmalny, K.; Mularski, J.; Ochodek, T.; Pawlak-Kruczek, H. Torrefaction and gasification of biomass for polygeneration: Production of biochar and producer gas at low load conditions. *Energy Rep.* **2022**, *8*, 134–144. [CrossRef]
39. Čespiva, J.; Skřínský, J.; Vereš, J.; Wnukowski, M.; Serenčíšová, J.; Ochodek, T. Solid recovered fuel gasification in sliding bed reactor. *Energy* **2023**, *278*, 127830. [CrossRef]
40. Han, S.W.; Lee, J.J.; Tokmurzin, D.; Lee, S.H.; Nam, J.Y.; Park, S.J.; Ra, H.W.; Mun, T.-Y.; Yoon, S.J.; Yoon, S.M.; et al. Gasification characteristics of waste plastics (SRF) in a bubbling fluidized bed: Effects of temperature and equivalence ratio. *Energy* **2022**, *238*, 121944. [CrossRef]
41. Aguado, R.; Escámez, A.; Jurado, F.; Vera, D. Experimental assessment of a pilot-scale gasification plant fueled with olive pomace pellets for combined power, heat and biochar production. *Fuel* **2023**, *344*, 128127. [CrossRef]
42. Basu, P. Chapter 7—Gasification Theory. In *Biomass Gasification, Pyrolysis and Torrefaction*, 3rd ed.; Academic Press: Cambridge, MA, USA, 2018; pp. 211–262.
43. DIN 51900-1; Determining the Gross Calorific Value of Solid and Liquid Fuels Using the Bomb Calorimeter, and Calculation of Net Calorific Value. Part 1: General Information. German Institute for Standardization: Berlin, Germany, 2000.
44. Cerone, N.; Zimbardi, F.; Contuzzi, L.; Baleta, J.; Cerinski, D.; Skvorčinskienė, R. Experimental investigation of syngas composition variation along updraft fixed bed gasifier. *Energy Convers. Manag.* **2020**, *221*, 113116. [CrossRef]
45. Knoef, H.A.M. *Handbook Biomass Gasification*; BTG Biomass Technology Group: Enschede, The Netherlands, 2005.
46. Karatas, H.; Akgun, F. Experimental results of gasification of walnut shell and pistachio shell in a bubbling fluidized bed gasifier under air and steam atmospheres. *Fuel* **2018**, *214*, 285–292. [CrossRef]
47. Cali, G.; Deiana, P.; Bassano, C.; Meloni, S.; Maggio, E.; Mascia, M.; Pettinau, A. Syngas production, clean-up and wastewater management in a demo-scale fixed-bed updraft biomass gasification unit. *Energies* **2020**, *13*, 2594. [CrossRef]
48. James, A.M.; Yuan, W.; Boyette, M.D.; Wang, D. The effect of air flow rate and biomass type on the performance of an updraft biomass gasifier. *BioResources* **2015**, *10*, 3615–3624. [CrossRef]
49. Hosseinzai, B.; Hadianfard, M.J.; Aghabarari, B.; García-Rollán, M.; Ruiz-Rosas, R.; Rosas, J.M.; Rodríguez-Mirasol, J.; Cordero, T. Pyrolysis of pistachio shell, orange peel and saffron petals for bioenergy production. *Bioresour. Technol. Rep.* **2022**, *19*, 101209. [CrossRef]
50. Dudek, M.; Adamczyk, B.; Grzywacz, P.; Lach, R.; Sitarz, M.; Lesniak, M.; Gajek, M.; Mech, K.; Wilk, M.; Rapacz-Kmita, A.; et al. The utilisation of solid fuels derived from waste pistachio shells in direct carbon solid oxide fuel cells. *Materials* **2021**, *14*, 6755. [CrossRef]

51. Deng, P.; Wan, W.; Azeem, M.; Riaz, L.; Zhang, W.; Yang, Y.; Li, C.; Yuan, W. Characterization of biochar derived from bamboo and its application to modulate the toxic effects of chromium on wheat plant. *Biomass Convers. Biorefinery* **2022**. [[CrossRef](#)]
52. Erbel, C.; Mayerhofer, M.; Monkhouse, P.; Gaderer, M.; Spliethoff, H. Continuous in situ measurements of alkali species in the gasification of biomass. *Proc. Combust. Inst.* **2013**, *34*, 2331–2338. [[CrossRef](#)]
53. Nowicki, P.; Bazan, A.; Kazmierczak-Razna, J.; Pietrzak, R. Sorption properties of carbonaceous adsorbents obtained by pyrolysis and activation of pistachio nut shells. *Adsorpt. Sci. Technol.* **2015**, *33*, 581–586. [[CrossRef](#)]
54. El-Bassi, L.; Ibn Ferjani, A.; Jeguirim, M.; Bennici, S.; Jellali, S.; Akrou, H.; Thevenin, N.; Ruidavets, L.; Muller, A.; Limousy, L. Production of a biofertilizer from exhausted grape marc waste: Agronomic and environmental impact on plant growth. *Biomass Convers. Biorefinery* **2022**, *12*, 5605–5618. [[CrossRef](#)]
55. Komnitsas, K.; Zaharaki, D.; Pyliotis, I.; Vamvuka, D.; Bartzas, G. Assessment of Pistachio Shell Biochar Quality and Its Potential for Adsorption of Heavy Metals. *Waste Biomass Valorization* **2015**, *6*, 805–816. [[CrossRef](#)]
56. Li, H.; Wang, B.; Siri, M.; Liu, C.; Feng, C.; Shao, X.; Liu, K. Calcium-modified biochar rather than original biochar decreases salinization indexes of saline-alkaline soil. *Environ. Sci. Pollut. Res.* **2023**, *30*, 74966–74976. [[CrossRef](#)]
57. Ge, S.; Wang, S.; Mai, W.; Zhang, K.; Tanveer, M.; Wang, L.; Tian, C. Characteristics and acidic soil amelioration effects of biochar derived from a typical halophyte *Salicornia europaea* L. (common glasswort). *Environ. Sci. Pollut. Res.* **2023**, *30*, 66113–66124. [[CrossRef](#)]
58. Demeyer, A.; Voundi Nkana, J.C.; Verloo, M.G. Characteristics of wood ash and influence on soil properties and nutrient uptake: An overview. *Bioresour. Technol.* **2001**, *77*, 287–295. [[CrossRef](#)]
59. Khiari, B.; Ghouma, I.; Ferjani, A.I.; Azzaz, A.A.; Jellali, S.; Limousy, L.; Jeguirim, M. Kenaf stems: Thermal characterization and conversion for biofuel and biochar production. *Fuel* **2020**, *262*, 116654. [[CrossRef](#)]
60. Peng, X.; Deng, Y.; Liu, L.; Tian, X.; Gang, S.; Wei, Z.; Zhang, X.; Yue, K. The addition of biochar as a fertilizer supplement for the attenuation of potentially toxic elements in phosphogypsum-amended soil. *J. Clean. Prod.* **2020**, *277*, 124052. [[CrossRef](#)]
61. Noori, M.; Zendehtel, M.; Ahmadi, A. Using natural zeolite for the improvement of soil salinity and crop yield. *Toxicol. Environ. Chem.* **2006**, *88*, 77–84. [[CrossRef](#)]
62. Parliament of the Czech Republic. *Government Regulation No. 75/2015 Coll., Government Regulation on the Conditions for the Implementation of Agri-Environmental-Climatic Measures and Amending Government Regulation No. 79/2007 Coll., on the Conditions for the Implementation of Agri-Environmental Measures, as Amended*; Parliament of the Czech Republic: Prague, Czech Republic, 2015.
63. Hornung, A.; Stenzel, F.; Grunwald, J. Biochar—Just a black matter is not enough. *Biomass Convers. Biorefinery* **2021**, *14*, 5889–5900. [[CrossRef](#)]
64. Tóth, G.; Hermann, T.; Da Silva, M.R.; Montanarella, L. Heavy metals in agricultural soils of the European Union with implications for food safety. *Environ. Int.* **2016**, *88*, 299–309. [[CrossRef](#)]
65. EBC. European Biochar Certificate—Guidelines for a Sustainable Production of Biochar. In *Carbon Standards International (CSI)*; Version 10.3; European Biochar Foundation (EBC): Arbaz, Switzerland, 2022.
66. Açıkalın, K.; Karaca, F.; Bolat, E. Pyrolysis of pistachio shell: Effects of pyrolysis conditions and analysis of products. *Fuel* **2012**, *95*, 169–177. [[CrossRef](#)]
67. Da Silva, J.C.G.; Alves, J.L.F.; Galdino, W.V.d.A.; Moreira, R.d.F.P.M.; José, H.J.; de Sena, R.F.; Andersen, S.L.F. Combustion of pistachio shell: Physicochemical characterization and evaluation of kinetic parameters. *Environ. Sci. Pollut. Res.* **2018**, *25*, 21420–21429. [[CrossRef](#)]
68. Ong, H.C.; Yu, K.L.; Chen, W.-H.; Pillejera, M.K.; Bi, X.; Tran, K.-Q.; Pétrissans, A.; Pétrissans, M. Variation of lignocellulosic biomass structure from torrefaction: A critical review. *Renew. Sustain. Energy Rev.* **2021**, *152*, 111698. [[CrossRef](#)]
69. Tavakoli Froushani, F.; Tavanai, H.; Hosseini, F.A. An investigation on the effect of KMnO_4 on the pore characteristics of pistachio nut shell based activated carbon. *Microporous Mesoporous Mater.* **2016**, *230*, 39–48. [[CrossRef](#)]
70. Niksiar, A.; Nasernejad, B. Activated carbon preparation from pistachio shell pyrolysis and gasification in a spouted bed reactor. *Biomass Bioenergy* **2017**, *106*, 43–50. [[CrossRef](#)]
71. Wu, F.-C.; Tseng, R.-L.; Juang, R.-S. Comparisons of porous and adsorption properties of carbons activated by steam and KOH. *J. Colloid Interface Sci.* **2005**, *283*, 49–56. [[CrossRef](#)]
72. Wu, F.-C.; Tseng, R.-L.; Hu, C.-C. Comparisons of pore properties and adsorption performance of KOH-activated and steam-activated carbons. *Microporous Mesoporous Mater.* **2005**, *80*, 95–106. [[CrossRef](#)]
73. Lua, A.C.; Yang, T.; Guo, J. Effects of pyrolysis conditions on the properties of activated carbons prepared from pistachio-nut shells. *J. Anal. Appl. Pyrolysis* **2004**, *72*, 279–287. [[CrossRef](#)]
74. Foo, K.Y.; Hameed, B.H. Preparation and characterization of activated carbon from pistachio nut shells via microwave-induced chemical activation. *Biomass Bioenergy* **2011**, *35*, 3257–3261. [[CrossRef](#)]
75. Aghbashlo, M.; Hosseinzadeh-Bandbafha, H.; Shahbeik, H.; Tabatabaei, M. The role of sustainability assessment tools in realizing bioenergy and bioproduct systems. *Biofuel Res. J.* **2022**, *9*, 1697–1706. [[CrossRef](#)]

Disclaimer/Publisher’s Note: The statements, opinions and data contained in all publications are solely those of the individual author(s) and contributor(s) and not of MDPI and/or the editor(s). MDPI and/or the editor(s) disclaim responsibility for any injury to people or property resulting from any ideas, methods, instructions or products referred to in the content.